



Available online at:

<http://www.italian-journal-of-mammalogy.it/article/view/11465/pdf>

doi:10.4404/hystrix-26.2-11465

Research Article

A lynx natural brain endocast from Ingarano (Southern Italy; Late Pleistocene): Taphonomic, Morphometric and Phylogenetic approaches

Dawid A. IURINO^{a,b,*}, Antonio PROFICO^{b,c}, Marco CHERIN^{b,d}, Alessio VENEZIANO^{b,e}, Loïc COSTEUR^{b,f}, Raffaele SARDELLA^{a,b}^aDipartimento di Scienze della Terra, Sapienza Università di Roma, Piazzale Aldo Moro 5, 00185, Rome, Italy^bPaleoFactory, Sapienza Università di Roma, Piazzale Aldo Moro 5, 00185, Rome, Italy^cDipartimento di Biologia Ambientale, Sapienza Università di Roma, Piazzale Aldo Moro 5, 00185 Roma, Italy^dDipartimento di Fisica e Geologia, Università degli Studi di Perugia, Via Alessandro Pascoli, 06123 Perugia, Italy^eSchool of Natural Sciences and Psychology, John Moores University, James Parsons Building, Byrom Street L3 3AF, Liverpool, United Kingdom^fNaturhistorisches Museum Basel, Augustinergasse 2, 4001 Basel, Switzerland**Keywords:**

Natural brain endocast
Carnivora
Felidae
Lynx
paleontology
geometric morphometrics
phylogenetic signal

Abstract

A natural brain endocast from the Late Pleistocene site of Ingarano (Apulia, Southern Italy) has been investigated in detail using CT scanning, image processing techniques and Geometric Morphometrics to obtain information about the taxonomy and taphonomy of the specimen. Based on its characteristically felid shape, we compared several measurements of the endocast with those of the brains of living Felidae, with a special emphasis on *Panthera pardus*, *Lynx lynx* and *Felis silvestris* earlier reported from the same locality. The applied combination of techniques revealed that this specimen is morphometrically closest to the brains of lynxes, and so can be reported as the first natural endocranial cast of Late Pleistocene *Lynx* sp. In addition, CT scanning of the Ingarano endocast allowed us to reconstruct the early stages of its taphonomy (i.e., the process of infilling of the braincase with the sediment).

Article history:

Received: 10 August 2015

Accepted: 10 December 2015

Acknowledgements

We gratefully thank all the people that helped and supported us in analysing museum collections: Dr. Rossella Carlini (Museo Civico di Zoologia di Roma), Prof. Augusto Vigna Taglianti (Sapienza University of Rome), Dr. Paolo Agnelli (Museo di Storia Naturale dell'Università degli Studi di Firenze). Dr. Massimiliano Danti and Prof. Sabino W. Della Sala (Ospedale M.G. Vannini) kindly provide access, assistance and facilities for the making of the CT scanning. LC thanks Georg Schulz and Bert Müller for the CT-scans at the Biomaterials Science Center of the University of Basel. Financial support of the Swiss National Science Foundation in the frame of the R'equip initiative (316030 133802) and of the Stiftung zur Förderung des Naturhistorischen Museums Basel is acknowledged. The authors also express their gratitude to Dr. Giovanni Amori, Dr. Dmitry V. Ivanoff and two anonymous reviewers who greatly improved this article with constructive comments and suggestions.

Introduction

The soft tissue traces of fossil mammals are exceptionally rare in the paleontological record and are mostly represented by natural brain casts, which are of great interest in paleontology (Moodie, 1922). Since one of the prime functions of the brain is collecting and processing sensory information, it represents a key organ for the interpretation of the sensory-perceptual ability in fossil vertebrates. Moreover, some of its features such as volume, shape and convolutions pattern can be analyzed for evolutionary purposes. The brain's cortical structures contact the endocranial vault and leave their imprints on the bone surface (Bruner, 2008). However, natural brain endocasts are rare because their genesis is possible only under highly specific sedimentary and diagenetic conditions (Hu et al., 2014). In fact, a natural brain endocast is a brain replica formed by the lithification of sediment that had filled the cranial cavity preserving the external cerebral and cerebellar morphology (Ivanoff et al., 2014). In the last two decades paleoneurological studies have largely used CT-scanning devices to obtain 3D virtual endocasts, thus considerably increasing the amount of anatomical and ecological information of fossils vertebrates (Orliac and Gilissen,

2012; Iurino et al., 2013; and references therein). Such technology allows obtaining high-resolution virtual 3D endocasts, rich in morphological details. Nevertheless, there are several limitations in obtaining high-quality virtual endocasts through tomographic techniques, which are due to the preservation status of the fossilized skulls (e.g., presence of fractures, missing portions and plastic deformations; Iurino et al., 2013). Some difficulties in the image processing may occur in relation to the type of fossilization (e.g., if the bone tissue or the sedimentary matrix in which the fossil is embedded are rich in metallic minerals, they can produce artefacts in tomographic images). In addition, CT and similar techniques require density differences between the bone and sediment to perform the surface extraction, otherwise it will not be possible to distinguish effectively the bone tissue from the sedimentary matrix (Abel et al., 2012; Iurino et al., 2013). On the other hand, some natural brain endocasts can preserve a comparable or even higher level of details than virtual endocasts produced by CT scans (Hu et al., 2014), resulting of great interest not only for paleoneurological studies but also for taphonomic and taxonomic purposes. The importance of both natural and virtual brain endocasts in paleontology is evidenced by decades of studies on this topic published by several authors (Moodie, 1922; Edinger, 1948; Dechaseaux, 1969; Jerison, 1975; Radinsky, 1978; Wang and Bao, 1984; Brochu, 2000; Kear, 2003; Takai et

* Corresponding author

Email address: dawid.iurino@uniroma1.it (Dawid A. IURINO)

al., 2003; Witmer et al., 2003; Kurochkin et al., 2007; Lyras, 2009; Gai et al., 2011; Sardella et al., 2014; Vinuesa et al., 2015a,b; among others). Despite the relative abundance of well-preserved *Lynx* fossils in the paleontological record (Werdelin, 1981; Cherin et al., 2013; Ghezzi et al., 2015), three-dimensionally preserved brain casts have never been documented before. Here we focus on the first natural brain endocast of Late Pleistocene *Lynx*. Using CT-based analyses, we explore the inner structure of the cast in order to obtain taphonomic information. In addition, through Geometric Morphometric analyses, we compare the digitalized specimen with virtual endocasts of extant mid-sized and large felids to test its taxonomic value.



Figure 1 – Location of the paleontological site of Ingarano (Foggia, South Italy).

Geological and paleontological framework

The Late Pleistocene fossiliferous site of Ingarano is a cave deposit located in an abandoned quarry near the town of Apricena (Foggia, South Italy) at about 270 m a.s.l. (Fig. 1). The deposit was discovered in 1985, but only in 1992 a general study was carried out. Radiometric analyses based on the $^{239}\text{Th}/^{234}\text{U}$ method provided an age of 40.000 ± 2.000 years BP (Capasso Barbato et al., 1992; Bedetti and Pavia, 2007). The rich vertebrate fauna from this site was studied by several authors (Capasso Barbato et al., 1992; Petronio et al., 1996; Petronio and Sardella, 1998; Curcio et al., 2005; Bedetti and Pavia, 2007; Iurino, 2014) and includes the following 42 species: Amphibians: *Rana* sp.; Reptiles: *Lacerta* sp.; Birds: *Circus aeruginosus*, *Buteo rufinus*, *Aquila chrysaetos*, *Falco columbarius*, *Falco cherrug*, *Alectoris graeca*, *Perdix perdix*, *Columba livia*, *Otus scops*, *Nyctea scandiaca*, *Nyctea scandiaca* vel *Bubo bubo*, *Athene noctua noctua*, *Pyrhocorax graculus*, *Pyrhocorax pyrrhocorax*, *Corvus corone*, *Corvus corone* vel *Corvus frugilegus*, *Corvus corax*; Mammals: *Erinaceus europaeus*, *Myothis blythi*, *Oryctolagus cuniculus*, *Lepus europaeus*, *Microtus* sp., *Microtus* gr. *arvalis/agrestis*, *Terricola savii*, *Apodemus sylvaticus*, *Elyomys quercinus*, *Canis lupus*, *Vulpes vulpes*, *Ursus arctos*, *Mustela nivalis*, *Martes* sp., *Meles meles*, *Gulo gulo*, *Crocuta crocuta*, *Felis silvestris*, *Lynx lynx*, *Panthera pardus*, *Equus hydruntinus*, *Cervus elaphus*, *Dama dama*, *Capreolus capreolus*, *Rupicapra* sp., *Bos primigenius* (Bedetti and Pavia, 2007; Iurino, 2014). Moreover, remains of *Panthera spelaea*, *Hippopotamus amphibius*, *Coelodonta antiquitatis*, *Stephanorhinus hemitoechus* and *Palaeoloxodon antiquus* were collected in a sandy-clay level having unclear stratigraphic relationships with the aforementioned karst deposit (Petronio and Sardella, 1998). Finally, Mousterian artifacts were found in the lower part of the section (Petronio et al., 1996). A large amount of specimens referable

to different species of carnivores are documented at Ingarano, in particular from the lower part of the deposit (levels C-D in Bedetti and Pavia, 2007). Well-preserved and complete skulls and mandibles were found, together with many limb bones, partially articulated. All the Carnivora that occurred in the Italian Peninsula during the Late Pleistocene are recorded at Ingarano, although the richest sample is that of lynx, wolf and red fox. A detailed taphonomic analysis of the assemblage is still in progress, but the abundance of well-preserved carnivore fossils suggests that the lower part of the deposit (levels C-D in Bedetti and Pavia, 2007) could be related to the presence of a natural trap.

Materials and methods

Studied material

The fossil described herein was discovered in 1989, during a field survey in the quarries of the Ingarano area by a research team of the Earth Sciences Department of Sapienza University of Rome, where the specimen is housed to date with the catalogue number ING 1989/13. The comparative sample consists of 19 specimens belonging to 13 extant species of Felidae as reported in Tab. A1.

CT-scanning

Tomographic images for most of the specimens were taken using a Philips Brilliance CT 64-channel scanner at M.G. Vannini Hospital (Rome). Both ING 1989/13 and the crania of extant felids were scanned in their entirety in the coronal (i.e., transverse for some authors) slice plane from front to back. The scanning resulted in 160 slices for ING 1989/13, with standard dimensions of 512×512 pixels (see Tab. A1 for the complete dataset of the comparative sample). The slice thickness of most of the specimens is 0.8 mm and the interslice space (i.e., the space between consecutive slices) is 0.4 mm. Image processing and 3D rendering of the specimens were computed using the open-source software OsiriX (version 5.6 32-bit).

Biometric analysis

Despite the absence of some portions of the endocast, several measurements were taken (Fig. 2) and compared with those of a few selected felids. The comparative sample included three felid species occurring in the Ingarano site according to Bedetti and Pavia (2007): *Lynx lynx*, *Panthera pardus* and *Felis silvestris*. However, ongoing unpublished research seems to indicate that some of these taxonomic attributions should be revised and that other felid taxa, namely *Felis silvestris lybica*, *Felis chaus* and *Lynx pardinus*, could have occurred at Ingarano. For this reason we also included these three taxa in the comparative sample (Tab. A1).

Geometric Morphometrics

The morphology of the fossil endocast from Ingarano was compared with a sample of 19 endocasts acquired through 3D virtual segmentation using the software Mimics (version 10.01). For each specimen a 3D set of 14 landmarks (Fig. 3) was recorded using the software Amira (version 5.4.5); the information about the definition of the landmark set is reported in Fig. 3. Since the endocast from Ingarano is partially incomplete, it was not possible to acquire a fully bilateral landmark configuration. The 20 sets of 14 landmarks were superimposed by a Generalized Procrustes Analysis (GPA; Zelditch et al., 2012). The GPA was performed using the function procSym of the Morpho package (Schlager, 2013). The Procrustes 3D coordinates were used to perform a Principal Component Analysis (PCA) and the variable Centroid Size (CS) was calculated for each landmark set. The amount of phylogenetic signal (Adams et al., 2013) in the morphometric data was assessed using a phylogenetic tree obtained from molecular data (Arnold et al., 2010). This signal was estimated by calculating both Blomberg's K (Blomberg et al., 2003) and Pagel's λ (Pagel, 1999). λ is a scaling parameter that measures the correlations between species, in relation to what is expected under Brownian evolution: λ is equal to 0 if there is no correlation between species and Brownian expectation and it is equal to 1.0 in the case of a perfect correlation. For Blomberg's K,

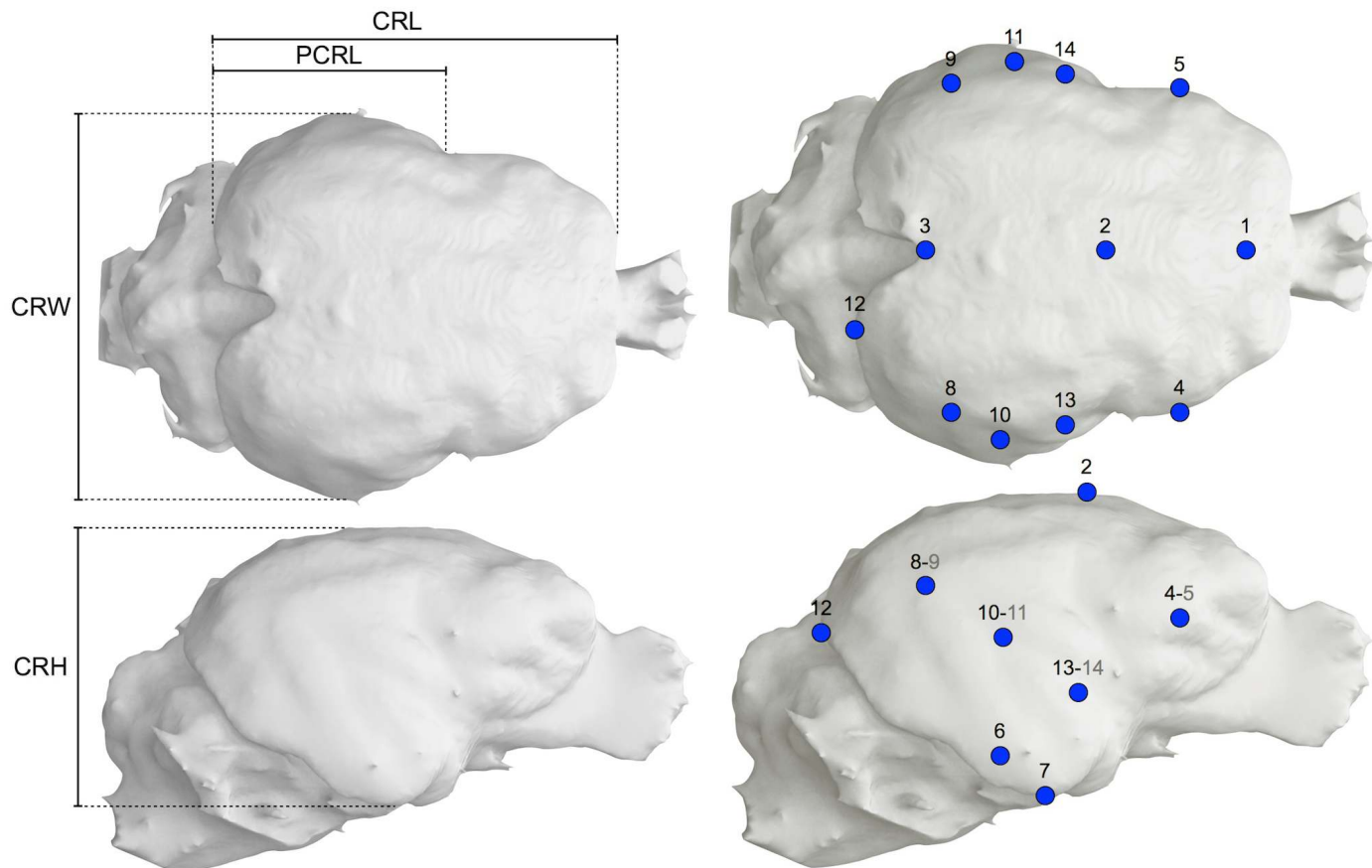


Figure 2 – Selected brain measurements used in the comparative analyses illustrated on a virtual endocast of *Lynx lynx*. Abbreviations: CRH, maximum height of cerebral cast; CRL, maximum length of cerebral cast exclusive of olfactory bulbs; CRW, maximum width of cerebral cast; PCRL, maximum length of posterior cerebral region.

values lower than 1.0 indicate that related species resemble each other less than expected under the Brownian motion model of trait evolution, and values greater than 1.0 imply that more related species are more similar than predicted by this model (Diniz-Filho et al., 2012). The phylogenetic signal was calculated on shape (PC scores) and size (CS) by using the “geomorph” and “phytools” R packages (Adams and Otárola-Castillo, 2005; Revell, 2012). In addition, a discriminant analysis on CS (i.e., the square root of the sum of squared distances of a set of landmarks from their centroid) was performed in order to understand whether it is possible to rely on size for assigning a brain endocast to its taxonomic allocation (genus).

Description and comparison

The natural brain endocast ING 1989/13 is well preserved except for the loss of the anterior portion of the right hemisphere, the basal portion of the left hemisphere and the cerebellum (Fig. 4 and A1). ING 1989/13 is 65.15 mm long and 59.66 mm wide and has a maximum height of 45.96 mm. The intact surface of the cast is covered by a thin layer (about 1 mm) of calcium carbonate, while the damaged surface exposes heterogeneous sediment with variable granulometry. This indicates that the missing portions were lost after the fossilization process has occurred. Judging from their reddish-brown color, both the surface and the inner portion of the cast are rich in iron oxides. There are few small fragments of fossilized bone tissue scattered on the cast surface and in particular in the caudal portion where a fragment of the tentorium is clearly visible in ventral view (Fig. 4b). The basal portion of the olfactory bulbs is still present although their anterior portion is missing (Fig. 4b-d). In dorsal view the sulcal morphology is recognizable on both sides, although the cruciate sulcus, the posterior sigmoid gyrus, the postcruciate sulcus and the coronal sulcus are present only on

Number	Side	Position
1	mid-sagittal	Meeting point between the longitudinal fissure and the posterior sigmoid gyrus
2	mid-sagittal	Vertex of the endocast along the midsagittal plane
3	mid-sagittal	Meeting point between the occipital gyri along the midsagittal plane
4-5	right-left	Most lateral point on the frontal lobe in dorsal view of the endocast
6	right	Most lateral point on the temporal lobe in dorsal view of the endocast
7	right	Lowest point on the temporal lobe
8-9	right-left	Point of maximum curvature on suprasylvian girus
10-11	right-left	Point of maximum curvature on ectosylvian girus
12	right	Most posterior point on occipital gyrus in dorsal view of the endocast
13-14	right-left	Deepest point of sylvian sulcus

Figure 3 – Configuration and description of landmarks used in this study shown on a virtual endocast of *Lynx lynx* in dorsal (top) and right lateral (below) views .

the left hemisphere, while the postlateral sulcus and occipital gyrus are better recognizable on the right hemisphere (Fig. 4c-d and 5a-c). The globose shape of ING 1989/13 and the general pattern of convolutions resemble those of an adult lynx (Fig. 5 and Tab. A1). According to Radinsky (1975) the postlateral sulcus overlaps with the lateral sulcus in *Lynx rufus*, *Lynx canadensis* and *Lynx lynx* with some exceptions. In ING 1989/13 and in our comparative sample of lynxes, including *Lynx pardinus*, this overlapping is not present, and the postlateral sulcus ends close to the caudal margin of the lateral sulcus (Fig. 5a). In most species of felids, the orbital sulcus is continuous with the anterior ectosylvian sulcus, while in lynxes the orbital sulcus seems to have an interruption (see Radinsky, 1975). The latter morphology is evident in our comparative sample of extant lynxes as well as on the left side of

ING 1989/13 (Fig. A1). In dorsal view, ING 1989/13 and *L. pardinus* show a short transverse sulcus (Fig. 5a and A1) reported by Radinsky (1975) also for *L. canadensis* and *L. lynx*, but not clearly visible in our sample of *L. lynx* and not present in other felids.

Results

Inner morphology

CT-scanning analyses were performed in order to obtain additional information about the taphonomic processes that gave rise to the natural endocast from Ingarano. Through the virtual segmentation of the digitalized specimen (Fig. 6) it was possible to observe the inner structure, and in particular the granulometry and arrangement of the sediment. The threshold value of the density was set to highlight the material with higher density (Fig. 6c-d). In addition, a density filter was applied to better discriminate the objects with different densities (Fig. 6e-f). The CT images confirm the non-homogeneous nature of the filling sediment (see Description and comparison), which is characterized by the presence of several rounded pebbles of millimeter to centimeter size. In dorsal view, these pebbles are concentrated mainly in the preserved anterior portion of the left hemisphere. In lateral view, the CT images show a stratification of the sediment into three distinct layers from top to bottom of the endocast (Fig. 6f). The top layer, with a maximum thickness of 16.05 mm, consists of larger granules ranging from 11.2 to 0.21 mm and is present in the frontal portion of the brain cast. The middle layer, with a maximum thickness of 15.35 mm, consists of a homogeneous sedimentary matrix with a few granules less than 0.2 mm in size. The bottom layer, with a maximum thickness of 14.56 mm, is rich in granules ranging from 0.66 to 0.12 mm and located mainly along the basal portion of the temporal lobes (Fig. 6f). The sedimentary matrix of the top layer shows a very low density, probably because of the presence of the large pebbles which allow the x-rays to cross the matrix with little attenuation.

Biometric and Geometric Morphometric analyses

The specimen ING 1989/13 resembles the lynx cerebrum in all the selected measurements, while it is significantly smaller than that of *P. pardus* and larger than that of the examined members of *Felis* (Tab. 1). The results of the Geometric Morphometric analysis confirm what has

been obtained by the biometric analysis. In the morphospace the specimen from Ingarano lies close to the range delimited by living representatives of the genus *Lynx*. As shown in Fig. 7, three nonoverlapped clusters are recognizable, corresponding to the genera *Felis*, *Lynx* and *Panthera*. The forms of *Puma concolor* and *Acinonyx jubatus* are located inside or at least very close to the *Panthera* variability range, while *Leptailurus serval* is positioned in the plot between the *Felis* and *Lynx* morphological ranges. The distribution of specimens along the PC1 is correlated to the CS. Indeed, the linear regression performed on these variables underlines an allometric pattern of variation in shape ($R^2=0.63$; p.value <0.01; slope =-0.21). The boxplot of the CS compiled per genus confirms the dimensional affinity between the Ingarano endocast and the brains of living lynxes (Fig. 8). In order to assess if the results of PCA and CS data can be used as phylogenetic indicators, we performed a phylogenetic test on the matrix of PC-scores averaged per species (only for the living species) and on CS (Fig. 9). The K statistics calculated for the entire morphology (i.e., all the principal components) shows a phylogenetic signal of 0.60. The K and λ parameters estimated for size (CS) indicate a high phylogenetic signal for this single trait when Brownian motion model of evolution is considered. K is higher than 1.0 (Tab. 1) and underlines a good fit between the size data and the phylogenetic differences between species. Similar results were obtained using Pagel's λ . The discriminant analysis confirms the pattern highlighted by the phylogenetic signal, giving a misclassification error of 0.22. A confusion matrix of the results is shown in Tab. A2.

Discussion

Taphonomy

In the last decades, a large amount of taphonomic data about soft tissue traces of fossil vertebrates were obtained through CT analysis (see Iurino et al., 2014; and references therein). The information derived from both the internal and external observations allow us to assume that the natural endocast ING 1989/13 originated in three different steps. Probably, the whole cranium or at least its neurocranial portion was intact during the burial process because of the integrity of the cast. The cranium was placed upside down, with the foramen magnum facing upward. This position is compatible with the distribution of the larger pebbles along the dorsal portion of the brain cavity during the first filling event. The energy of the flow was sufficiently high to allow the transport of these granules together with a large amount of silt. During the deposition process, the heavier objects settled on the bottom by the effect of gravity, while the silty matrix and the smaller clasts filled the brain cavity for more than half of its height. According to this interpretation the above-mentioned event did not occlude the foramen magnum. This allowed a second filling event, which occurred at a later stage and filled the remaining portion of the brain cavity with silty material rich in small limestone clasts. These two sedimentation events are compatible with the stratification observable from the tomographic images (Fig. 6f) and explain its origin (i.e., the top and middle layers pertain to the first filling event, while the bottom layer to the second one). The last step is represented by the formation of a thin carbonate crust that wrapped the entire content of the brain cavity. This probably occurred after a slight volume reduction of the brain endocast due to dehydration, when percolating water filled the very thin interstice area between the endocast and the inner braincase, depositing calcium carbonate. This crust contributed to strengthen the endocast and to preserve the details of its external anatomy. Moreover, the remains of the tentorium (Fig. 4b) suggest that a physical, not chemical, removal of the cranial bones occurred after the formation process of the natural endocast.

Taxonomy

Natural brain endocasts offer much evidence to understand the evolution of the central nervous system and to infer the sensory-perceptual abilities in fossil vertebrates. The main problem of an isolated natural brain endocast, devoid of any diagnostic cranial portion, is the difficulty in its taxonomic attribution. It is therefore necessary to identify

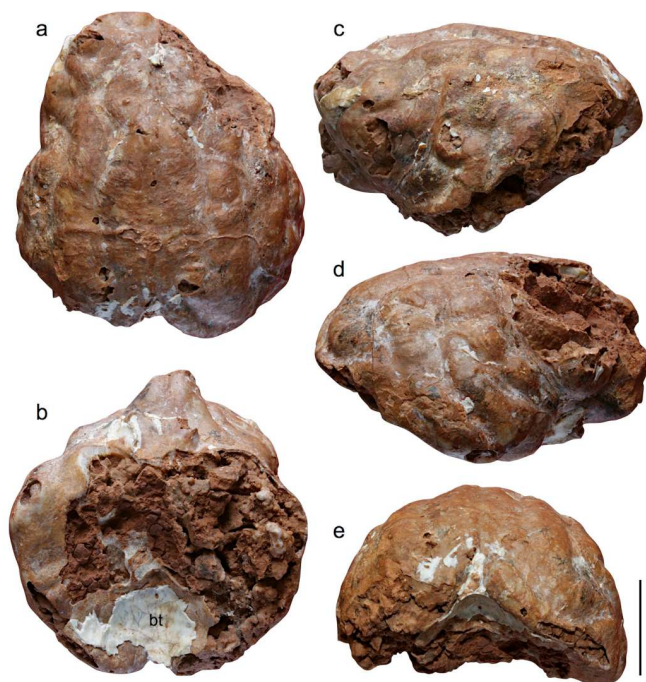


Figure 4 – The natural brain endocast of *Lynx* sp. (Ingarano, Italy, ING 1989/13) in dorsal (a), ventral (b), left lateral (c), right lateral (d) and caudal (e) views. Bone tissue (bt). Scale bar 2 cm.

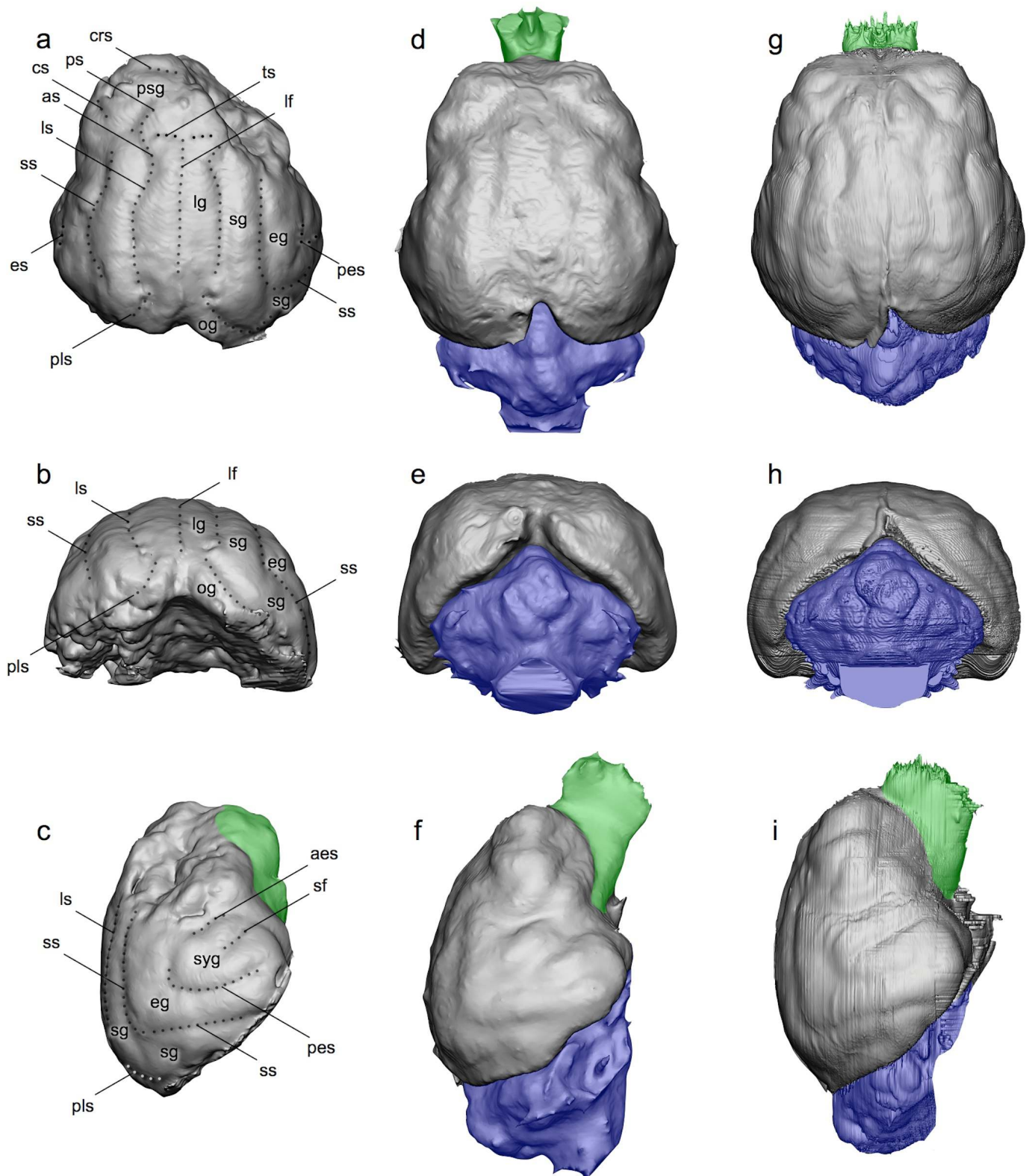


Figure 5 – Virtual endocast ING 1989/13 (a-c) compared to those of extant *Lynx lynx* PR 8 (d-f) and *Lynx pardinus* NMB 8865 (g-i). All specimens are in dorsal (a, d, g), caudal (b, e, h) and right lateral (c, f, i) views. Abbreviations: aes, anterior ectosylvian sulcus; as, ansate sulcus; crs, cruciate sulcus; cs, coronal sulcus; eg, ectosylvian gyrus; lf, longitudinal fissure; lg, lateral gyrus; ls, lateral sulcus; og, occipital gyrus; pes, posterior ectosylvian sulcus; pls, postlateral sulcus; ps, posteruciate sulcus; psg, posterior sigmoid gyrus; sf, sylvian fissure; sg, suprasylvian gyrus; ss, suprasylvian sulcus; syg, sylvian gyrus; ts, transverse sulcus. Olfactory bulbs and peduncles in green, cerebellum and spinal cord in violet. The images are normalized.

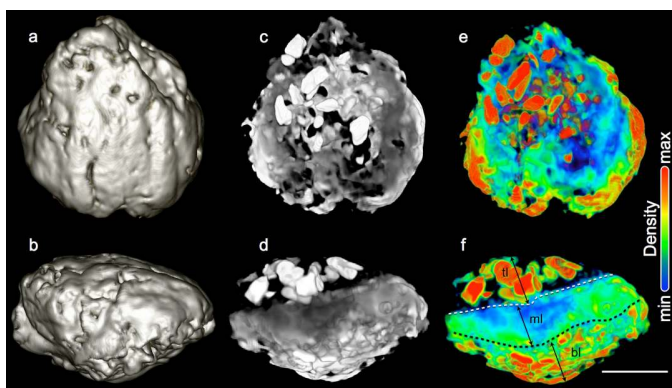
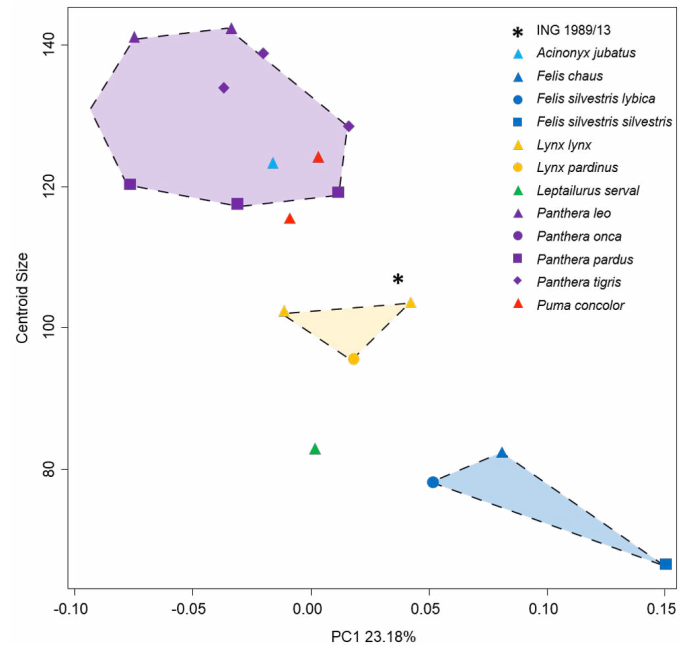
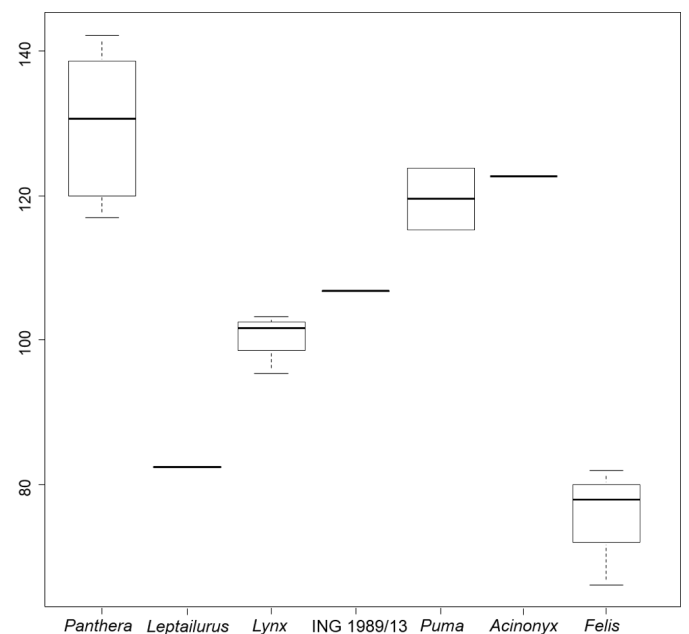
Table 1 – Brain endocast measurements (mm) of ING 1989/13 and extant *Lynx lynx*, *Lynx pardinus*, *Panthera pardus*, *Felis silvestris silvestris*, *Felis silvestris lybica* and *Felis chaus*.

	ING 1989/13	<i>Lynx lynx</i> (MC 85)	<i>Lynx lynx</i> (PR 8)	<i>Lynx pardinus</i> (NMB 8865)	<i>Panthera pardus</i> (MC 381)	<i>Felis silvestris silvestris</i> (84)	<i>Felis silvestris lybica</i> (C.2114)	<i>Felis chaus</i> (C.12308)
CRL	65.15	62.12	62.13	58.33	72.86	43.61	36.88	49.57
PCRL	38.74	39.61	39.33	36.85	53.03	29.18	24.62	36.18
CHR	45.96	48.88	47.53	42.12	54.74	34.41	27.77	37.94
CRW	59.66	58.97	58.87	53.84	66.49	43.96	38.46	47.28

Table 2 – Results of phylogenetic signal calculated for the overall shape, PC1, PC2 and CS. Columns include values of Blomberg's K, Pagel's λ , logL, logL0 (total absence of phylogenetic signal) and logL1 (complete correlation with phylogenetic tree tested).

	λ	K	logL	logL0	logL1
Shape	-	0.6	-46.9	-	-
PC1	0.00041	0.5	40.22	40.22	37.83
PC2	0.00041	0.63	30.98	30.98	29.86
CS	1.14	1.3	-46.75	-49.84	-46.92

features of taxonomic value in the external morphology and size (or in both). According to our biometric and Geometric Morphometric analyses, the size and the rounded shape of ING 1989/13 are compatible with the brain proportions of a middle-sized felid. As a matter of fact, the brain morphology of other carnivores from the Ingarano site such as canids and hyaenids, is significantly different from that of felids in having a more elongated cerebrum, with a different sulcal pattern and differently shaped olfactory bulbs (Radinsky, 1969). The results of the biometric comparison led us to exclude that the brain endocast from Ingarano might represent the genera *Panthera* and *Felis*, because of the significantly different cerebrum size (Fig. 7, 8 and Tab. 1). The lynx is the only medium sized felid found in the Ingarano site and we can undoubtedly attribute the brain endocast to this taxon. The results of the phylogenetic comparisons demonstrate the potential of size for the taxonomic identification of an individual brain endocast. Also, the discriminant function analysis confirms this conclusion and demonstrates that the overall size of the brain in felids is a good indicator of the Operational Taxonomic Unit (OTU; at the genus level in this study). Moreover, the size and pattern of convolutions of ING 1989/13 are compatible with those of an adult lynx (Fig. 5), as suggested by the results of the biometric and Geometric Morphometric analyses (Fig. 7, 8 and Tab. 1). It is clear from our quantitative analyses (Fig. 7, 8 and Tab. 1), that the specimen ING 1989/13 is closest to the brains of *Lynx*. According to the faunal lists reported by several authors (Capasso Barbato et al., 1992; Petronio et al., 1996; Petronio and Sardella, 1998; Curcio et al., 2005; Bedetti and Pavia, 2007), all the lynx remains from

**Figure 6** – CT images of the natural brain endocast ING 1989/13 of *Lynx* sp.. External surface in dorsal (a) and left lateral (b) views; inner morphology in dorsal (c) and left lateral (d) views; inner morphology with density filter applied in dorsal (e) and left lateral (f) views. Top layer (tl), middle layer (ml), bottom layer (bl). The black and white dotted lines in f separate the three different sediment layers, while the black double arrows indicate the maximum thickness of each layer. Scale bar 2 cm.**Figure 7** – Scatterplot of the first principal component and centroid size. Dashed lines border the specimens belonging to the same genus.**Figure 8** – Boxplot of the centroid size of ING 1989/13 and the comparison sample pooled by genus.

Ingarano are referred to the species *Lynx lynx*, but a detailed analysis of Late Pleistocene lynxes from Southern Italy is really needed to provide a firm taxonomical attribution. For now, the possible attribution of this material to other similar taxa, such as the Iberian lynx *Lynx pardinus* (Boscaini et al., 2015) and the cave lynx *Lynx spelaeus* (or *L. pardinus*

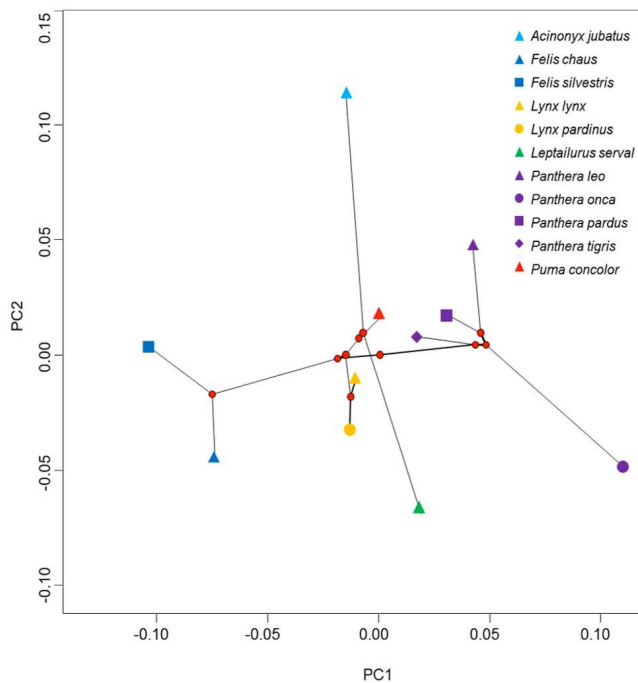


Figure 9 – Plot of the phylogenetic tree (nodes shown as red circles) and the set of Procrustes-aligned specimens in tangent space of the first two dimensions.

spelaeus; see below), cannot be excluded. The debate on the taxonomy and paleobiogeographic distribution of Late Pleistocene lynxes in Italy is still in progress (see Ghezzi et al., 2015; and references therein). Several authors (see Cherin et al., 2013; and references therein) accept the evolution of *L. pardinus* in Europe and *L. lynx* in Asia from the common ancestor *L. issiodorensis*. Nevertheless, many questions remain unresolved to date. In particular, the taxonomy of the so-called “cave lynx” is controversial. Many authors consider *L. spelaeus* as a subspecies and probable ancestor of the Iberian lynx *L. pardinus*, following the anagenetic evolutionary model first proposed by Werdelin (1981). According to this model, the extinct *L. issiodorensis* (which is very well represented in the Italian fossil record; Cherin et al., 2013) gave rise to *L. pardinus* through an intermediate form, namely *L. p. spelaeus*. On the other hand, other researchers consider *L. spelaeus* as a distinct fossil species, which was found mainly in Middle-Late Pleistocene cave sites of Southern France and Northern Italy (Bonifay, 1971; Rustioni et al., 1995; Testu, 2006; Ghezzi et al., 2015). It is generally accepted that the Eurasian lynx *L. lynx* spread to Europe from Asia during the Eemian interglacial period (130–115 ka; Werdelin, 1981), but its taxonomic and paleobiogeographic relationships with the preexisting lynx species, such as the “cave lynx”, are uncertain. Recent analysis based on ancient DNA (Rodríguez-Varela et al., 2015) highlighted the co-occurrence of the Iberian lynx and Eurasian lynx in the locality of Arene Candide (North Italy) during the Last Glacial Maximum. However, there are still no reports of paleontological remains of the Iberian lynx in other parts of Italy. The large sample of *Lynx* specimens from Ingarano could contribute to solve some of the aforementioned problems. Our results do not allow classifying ING 1989/13 at the species level, because both the size and morphology of the brain endocast do not provide sufficient diagnostic evidence. For this reason, the Ingarano specimen is identified as *Lynx* sp. Nevertheless, although not exhaustive, this study was successful in tracing the taxonomy – even if only at the genus level – of a fossil mammal from the Italian Pleistocene starting from the analysis of an isolated brain cast, thus contributing to the methodological basis for addressing other similar case studies. Further research on the rich cranial and postcranial sample from Ingarano will be of crucial importance to clarify the taxonomy of this felid and to depict the spread and the evolution of *Lynx* in the Late Pleistocene of Italy. ☞

References

- Abel R.L., Laurini C.R., Richter M., 2012. A palaeobiologist's guide to 'virtual' micro-CT preparation. *Palaeontol. Electron.* 15(2): 6T,17p. palaeo-electronica.org/content/issue-2-2012-technical-articles/233-micro-ct-workflow
- Adams D.C., Otárola-Castillo E., 2005. Geomorph: an R package for the collection and analysis of geometric morphometric shape data. *Methods Ecol. Evol.* 4(4): 393–399.
- Adams D.C., Rohlf F.J., Slice D.E., 2013. A field comes of age: geometric morphometrics in the 21st century. *Hystrix* 24(1): 7–14. doi:10.4404/hystrix-24-1-6283
- Arnold C., Matthews L.J., Nunn C.L., 2010. The 10kTrees website: a new online resource for primate phylogeny. *Evolutionary Anthropology: Issues, News, and Reviews* 19(3): 114–118.
- Bedetti C., Pavia M., 2007. Reinterpretation of the Late Pleistocene Ingarano cave deposit based on the fossil bird associations (Apulia, South-Eastern Italy). *Riv. Ital. Paleontol. S.* 113(3): 487–507.
- Blomberg S.P., Garland Jr.T., Ives A.R., 2003. Testing for phylogenetic signal in comparative data: behavioral traits are more labile. *Evolution* 57(4): 717–745.
- Bonifay M.F., 1971. Carnivores quaternaires du Sud-Est de la France. *Mém. Mus. Natl. Hist. Nat. N. S. Sér. C-21*(2): 43–377.
- Boscaini A., Madurell-Malapeira J., Llenas M., Martínez-Navarro B., 2015. The origin of the critically endangered Iberian lynx: speciation, diet and adaptive changes. *Quat. Sci. Rev.* 123: 247–253.
- Brochu C.A., 2000. A digitally-rendered endocast for *Tyrannosaurus rex*. *J. Vertebr. Paleontol.* 20(1): 1–6.
- Bruner E., 2008. Comparing endocranial form and shape differences in modern humans and Neandertal: A geometric approach. *PaleoAnthropology* 2008: 93–106.
- Capasso Barbato L., Cassoli P.F., Miniari M.R., Petronio C., Sardella R., Scaramo M., 1992. Note preliminari sulla fauna pleistocenica di Ingarano. *Boll. Soc. Paleontol. I.* 31(3): 325–334.
- Cherin M., Iurino D.A., Sardella R., 2013. New well-preserved material of *Lynx issiodorensis valdarnensis* (Felidae, Mammalia) from the Early Pleistocene of Pantalla (central Italy). *Boll. Soc. Paleontol. I.* 54: 103–111.
- Curcio M.T., Contoli L., Di Canzio E., Kotsakis T., 2005. Preliminary analysis of the first lower molar variability in Late Pleistocene and living population of *Terricola savii* (Arvicolidae, Rodentia). *Geo. Alp.* 2: 91–98.
- Dechaseaux C., 1969. Moulages endocrâniens d'artiodactyles primitifs, essai sur l'histoire du néopallium. *Annls. Paléont.* 55: 195–248.
- Diniz-Filho J.A.F., Santos T., Rangel, T.F., Bini L.M., 2012. A comparison of metrics for estimating phylogenetic signal under alternative evolutionary models. *Genet. Mol. Biol.* 35(3): 673–679.
- Edinger T., 1948. Evolution of the horse brain. *Geol. Soc. Am. Mem.* 25: 1–187.
- Gai Z., Donoghue P.C., Zhu M., Janvier P., Stambanoni M., 2011. Fossil jawless fish from China foreshadows early jawed vertebrate anatomy. *Nature* 476(7360): 324–327.
- Ghezzi E., Boscaini A., Madurell-Malapeira J., Rook L., 2015. Lynx remains from the Pleistocene of Valdeminio cave (Savona, Northwestern Italy), and the oldest occurrence of *Lynx spelaeus* (Carnivora, Felidae). *Rend. Fis. Acc. Lincei* 26: 87–95.
- Hu Y., Chen Y., Wang S., Sun Q., 2014. Pleistocene equid brain endocast from Shanxi Province, China. *Acta Palaeontol. Pol.* 59(2): 253–258.
- Iurino D.A., Danti M., Della Sala S.W., Sardella R., 2013. Modern techniques for ancient bones: Vertebrate Palaeontology and medical CT analysis. *Boll. Soc. Paleontol. I.* 52(3): 145–155.
- Iurino D.A., Bellucci L., Schreye D., Sardella R., 2014. Exceptional soft tissue fossilization of a Pleistocene vulture (*Gyps fulvus*): new evidence for emplacement temperatures of pyroclastic flow deposits. *Quat. Sci. Rev.* 96: 180–187.
- Iurino D.A., 2014. Body size reduction and teeth agenesis in Late Pleistocene *Meles meles* (Carnivora, Mammalia) from Ingarano (Southern Italy). *Riv. Ital. Paleontol. S.* 120(1): 109–118.
- Ivanoff D.V., Wolsan M., Marciszak A., 2014. Brainy stuff of long-gone dogs: a reappraisal of the supposed *Canis* endocranial cast from the Pliocene of Poland. *Naturwissenschaften* 101(8): 645–651.
- Jerison H.J., 1975. Fossil evidence of the evolution of the human brain. *Annu. Rev. Anthropol.* 4: 27–58.
- Kear B.P., 2003. Macropodoid endocranial casts from the early Miocene of Riversleigh, northern Queensland. *Alcheringa*. 27: 295–302.
- Klingenberg C.P., Gidaszewski N.A., 2010. Testing and quantifying phylogenetic signals and homoplasy in morphometric data. *Syst. Biol.* 59(3): 245–261.
- Klingenberg C.P., 2013. Visualizations in geometric morphometrics: how to read and how to make graphs showing shape changes. *Hystrix* 24(1): 15–24. doi:10.4404/hystrix-24-1-7691
- Kurochkin E.N., Dyke G.J., Saveliev S.V., Pervushov E.M., Popov E.V., 2007. A fossil brain from the Cretaceous of European Russia and avian sensory evolution. *Biol. Letters* 3: 309–313.
- Lyras G., 2009. The evolution of the brain in Canidae (Mammalia, Carnivora). *Scripta Geologica* 139: 1–93.
- Moodie R.L., 1922. On the endocranial anatomy of some Oligocene and Pleistocene mammals. *J. Comp. Neurol.* 34(4): 343–379.
- Orliac M.J., Gilissen, E., 2012. Virtual endocranial cast of earliest Eocene *Diacodexis* (Artiodactyla, Mammalia) and morphological diversity of early artiodactyl brains. *Proc. R. Soc. Lond. Biol.* 279: 3670–3677.
- Pagel M., 1999. Inferring the historical patterns of biological evolution. *Nature* 401(6756): 877–884.
- Petronio C., Billia E., Capasso Barbato L., Di Stefano G., Mussi M., Parry S.J., Sardella R., Voltaggio M., 1996. The late Pleistocene fauna from Ingarano (Gargano, Italy): biochronological, paleoecological, paleoethnological and geochronological implications. *Boll. Soc. Paleontol. I.* 34: 333–339.
- Petronio C., Sardella R., 1998. Remarks on the stratigraphy and biochronology of the late Pleistocene deposit of Ingarano (Apulia, Southern Italy). *Riv. Ital. Paleontol. S.* 104: 287–294.
- Radinsky L., 1969. Outlines of canid and felid brain evolution. *Ann. NY Acad. Sci.* 167(1): 277–288.
- Radinsky L., 1975. Evolution of the felid brain. *Brain, Behavior and Evolution* 11: 214–254.
- Radinsky L., 1978. Evolution of brain size in carnivores and ungulates. *Am. Nat.* 815–831.
- Revell L.J., 2012. Phytools: An R package for phylogenetic comparative biology (and other things). *Methods Ecol. Evol.* 3(2): 217–223.

- Rodríguez-Varela R., Tagliacozzo A., Ureña I., García N., Crégut-Bonnoure E., Mannino M.A., Arsuaga J.L., Valdiosera C., 2015. Ancient DNA evidence of Iberian lynx palaeoendemism. *Quat. Sci. Rev.* 112: 172–180.
- Rustioni M., Sardella R., Rook L. 1995. Note sulla distribuzione e sulla tassonomia del genere *Lynx* in Italia. *Padusa Quaderni* 1: 359–364.
- Sardella R., Bertè D., Iurino D.A., Cherin M., Tagliacozzo A., 2014. The wolf from Grotta Romanelli (Apulia, Italy) and its contribution in clarifying the evolutionary history of *Canis lupus* in the Late Pleistocene of southern Italy. *Quatern. Int.* 328: 179–195.
- Schlager S., 2013. Morpho: Calculations and visualizations related to Geometric Morphometrics. R package version. 0.23, 3.
- Takai M., Shigehara N., Egi N., 2003. Endocranial cast and morphology of the olfactory bulb of *Amphipithecus mogaungensis* (latest middle Eocene of Myanmar). *Primates* 44: 137–144.
- Testu A., 2006. Etude paléontologique et biostratigraphique des Felidae et Hyaenidae pléistocènes de l'Europe méditerranéenne. Ph.D. dissertation, Université de Perpignan.
- Vinuesa V., Madurell-Malapeira J., Fortuny J., Alba D.M., 2015a. The Endocranial morphology of the Plio-Pleistocene bone-cracking hyena *Pliocrocuta perrieri*: Behavioral implications. *J. Mamm. Evol.* 22(3): 421–434.
- Vinuesa V., Iurino D.A., Madurell-Malapeira J., Liu J., Fortuny J., Alba D.M., 2015b. Inferences of social behavior in bone-cracking hyaenids (Carnivora, Hyaenidae) based on digital paleoneurological techniques: Implications for human-carnivoran interactions in the Pleistocene. *Quatern. Int.* doi:10.1016/j.quaint.2015.10.037
- Wang J.W., Bao Y.C., 1984. A fossil brain of the large Felid from North Xizang. *Vertebrata Palasiatica* 22: 134–137.
- Werdelin L., 1981. The evolution of lynxes. *Ann. Zool. Fenn.* 18: 37–71.
- Witmer L.M., Chatterjee S., Franzosa J., Rowe T., 2003. Neuroanatomy of flying reptiles and implications for flight, posture and behaviour. *Nature* 425(6961): 950–953.
- Zelditch M.L., Swiderski D.L., Sheets H.D., 2012. *Geometric morphometrics for biologists: A primer*. Academic Press.

Associate Editor: D.G. Preatoni

Supplemental information

Additional Supplemental Information may be found in the online version of this article:

Figure S1 The natural brain endocast of *Lynx* sp. (Ingarano, Italy, ING 1989/13) in dorsal, ventral, left lateral, right lateral and caudal views.

Table S1 Dataset of the comparative sample.

Table S2 Confusion matrix used for the discriminant analysis.